A High-Resolution 3D Ultrasonic System for Rapid Evaluation of the Anterior and Posterior Segment

Gholam A. Peyman, MD; Charles P. Ingram, MS; Leonardo G. Montilla, BS; Russell S. Witte, PhD

■ **BACKGROUND AND OBJECTIVE:** Traditional ultrasound imaging systems for ophthalmology employ slow, mechanical scanning of a single-element ultrasound transducer. The goal was to demonstrate rapid examination of the anterior and posterior segment with a three-dimensional (3D) commercial ultrasound system incorporating high-resolution linear probe arrays.

■ **MATERIALS AND METHODS:** The 3D images of the porcine eye were generated in approximately 10 seconds by scanning one of two commercial linear arrays (25- and 50-MHz). Healthy enucleated pig eyes were compared with those with induced injury or placement of a foreign material (eg, metal). Rapid, volumetric imaging was also demonstrated in one human eye in vivo.

■ **RESULTS:** The 50-MHz probe provided exquisite volumetric images of the anterior segment at a depth up to 15 mm and axial resolution of 30 µm. The 25-MHz probe provided a larger field of view (lateral X depth: 20 × 30 mm), sufficient for capturing the entire anterior and posterior segments of the pig eye, at a resolution of 60 µm. A 50-MHz scan through the human eyelid illustrated detailed structures of the Meibomian glands, cilia, cornea, and anterior segment back to the posterior capsule.

■ **CONCLUSION:** The 3D system with its high-frequency ultrasound arrays, fast data acquisition, and volume rendering capability shows promise for investigating anterior and posterior structures of the eye.

[Ophthalmic Surg Lasers Imaging 2012;43:143-151.]

INTRODUCTION

Ultrasound technology was initially developed for military use and became useful in medicine[1,2] because of its ability to quickly image internal organs at low cost. Early pioneers in ophthalmic ultrasound introduced A-scan for ocular biometry and later for calculation of intraocular lens (IOL) power[3-8] and for differentiating solid from vas-

From the Department of Radiology (GAP, CPI, LGM, RSW), University of Arizona, Tucson; the Department of Basic Medical Sciences (GAP), University of Arizona, Phoenix Campus, Phoenix, Arizona; and the Department of Ophthalmology (GAP), Tulane University, New Orleans, Louisiana.

Originally submitted June 1, 2011. Accepted for publication October 28, 2011. Posted online January 12, 2012.
Presented at the American Society of Cataract and Refractive Surgery annual meeting, March 25-29, 2011, San Diego, California.
The authors have no financial or proprietary interest in the materials presented herein.
Address correspondence to Gholam A. Peyman, MD, 10650 Tropicana Circle, Sun City, AZ 85351. E-mail: gpeyman1@yahoo.com
doi: 10.3928/15428877-20120105-01

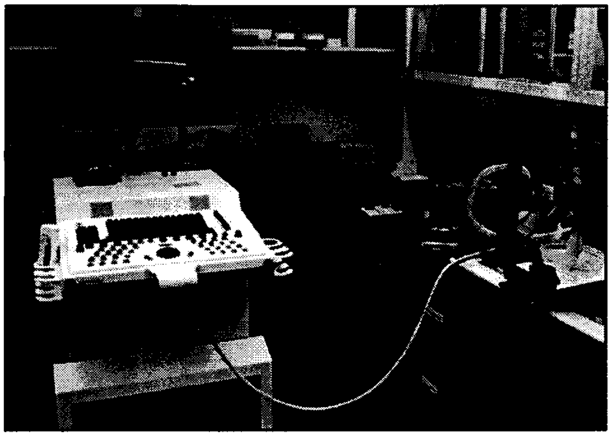

Figure 1. Photograph of the Vevo 2100 high-resolution ultrasound system (VisualSonics, Toronto, Ontario, Canada).

cular intraocular tumors.[9,10] B-scan ultrasound[11-17] generates two-dimensional (2D) images of the ocular, adnexal, and orbital structures and is an invaluable tool in clinical evaluation of eyes with opaque media and intraocular tumors.[18-27] These units can also be used in the emergency department to detect the extent of ocular trauma and location of intraocular foreign bodies.[28-31]

High-frequency B-scan ultrasound (50- to 100-MHz) using a handheld probe has been incorporated into commercial units. For example, the UBM (Paradigm Medical Industries Inc., Salt Lake City, UT) enables high axial resolution (20 µm) at a depth exceeding 4 mm.[32-35] Similarly, an arc-scanning high-resolution system (Artemis Inc., Cornell, NY, and ArcScan Inc., Evergreen, CO) is used to evaluate the anterior segment and as guidance during refractive surgery.[36-38] Both systems employ a single element oscillating transducer with a fixed depth of focus.

Shortcomings remain in current B-mode ultrasound images obtained in ophthalmology. In a routine contact B-mode sector scan without a water bath and an eyelid speculum,[16] the anterior segment remains blurred or cannot be imaged. The ciliary body structure cannot usually be seen using conventional 60° B-mode imaging generated by mechanical sector scan probes. For detailed examination of the posterior segment and the ciliary body, the ultrasonic probe needs to be positioned opposite the area of the globe and orthogonal to the region being examined. Because of these limitations, a complete ocular examination using contact B-scan ultrasound can be time-consuming, depending on the skill of the examiner. Time constraints limit the use of B-scan ultrasound in routine ophthalmic practice for examination of the anterior and posterior segments of the eye. This can lead to delay in recognizing early stage (small) neoplastic lesions involving the iris–ciliary body area. These lesions become visible only when their growth causes visual symptoms or they are discovered by chance when examined by a specialist. Moreover, ultrasound "C planes" (lateral or XY planes) can only be reviewed after producing volumetric ultrasound images, which, until recently, could only be acquired after slow mechanical scanning with a high-frequency, single-element transducer. Such slow scanning is typically not realistic in a clinical setting.

Recent developments in three-dimensional (3D) ultrasound and Doppler technology permit precise localization and volumetric measurement of ocular structures[39,40] and evaluation of blood flow.[41-48] However, 3D imaging with commercial systems is not common, and typically requires several minutes to produce a single 3D image.

In contrast to commonly used mechanical scanning of standard single-element transducers, high-frequency (> 20 MHz) linear ultrasonic arrays have not been readily available for ophthalmic applications.[49,50] Such arrays are made of 100 or more piezoelectric elements packed into the face of the transducer probe. The advantages of a high-frequency array for 2D or 3D imaging are significant in terms of spatial resolution and real-time imaging of the entire eye at different depths. Until recently, fabrication of high-frequency ultrasound arrays has been challenging due to small piezoelectric elements with narrow spacing. The size and spacing of piezoelectric crystals are inversely proportional to the generated ultrasound frequency.[51] New developments in ultrasound array fabrication technology using a patented technique of laser cutting have facilitated rapid or real-time scanning of the entire eye for ophthalmic applications.

The Vevo 2100 ultrasound system (VisualSonics, Toronto, Ontario, Canada) was developed for laboratory use in small animal body scanning. We believe our preliminary evaluation of the Vevo 2100—with its high-frequency ultrasound arrays and fast imaging and volume rendering capabilities—provides the impetus for larger scale investigation of its potential for examination of anterior and posterior structures in ophthalmic practice.

PATIENTS AND METHODS

Instrumentation

The Vevo 2100 at the University of Arizona is equipped with high-frequency transducers MS250 (13 to

24 MHz) and MS550D (22 to 55 MHz) (Figs. 1 and 2). Each solid-state transducer is composed of a 256-element linear array. The MS250 and MS550D have axial resolutions of 60 and 22 µm, respectively, at their focal depth. Unlike the older Vevo 770 system, the new system employs ultrasound probes capable of electronic transmit and receive beam forming such that most of the image remains in focus. Information received by these transducers is stored and processed to create real-time 2D images. Volumetric images can be generated in seconds with a simple linear translation of the probe in the elevational direction.

Although the Vevo system was originally designed for small animal imaging (eg, mice, rats, and zebra fish), its applications have extended to the clinic for microsurgery and other applications that benefit from the same high-resolution ultrasound arrays (more than eight standard probes are currently offered by VisualSonics). The 25-MHz probe (MS250) has a field of view up to 23 × 30 mm (width × depth) with B-mode frame rates greater than 100 Hz. The higher resolution 50-MHz probe (MS550D) has a field of view up to 14 × 15 mm, also with frame rates greater than 100 Hz. The system can operate in a variety of imaging modes including B-mode, M-mode, PW Doppler, 3D-mode, Color Doppler, Power Doppler, Tissue Doppler, Contrast Mode, and Photoacoustic Imaging. The 3D-mode uses a mechanical motor

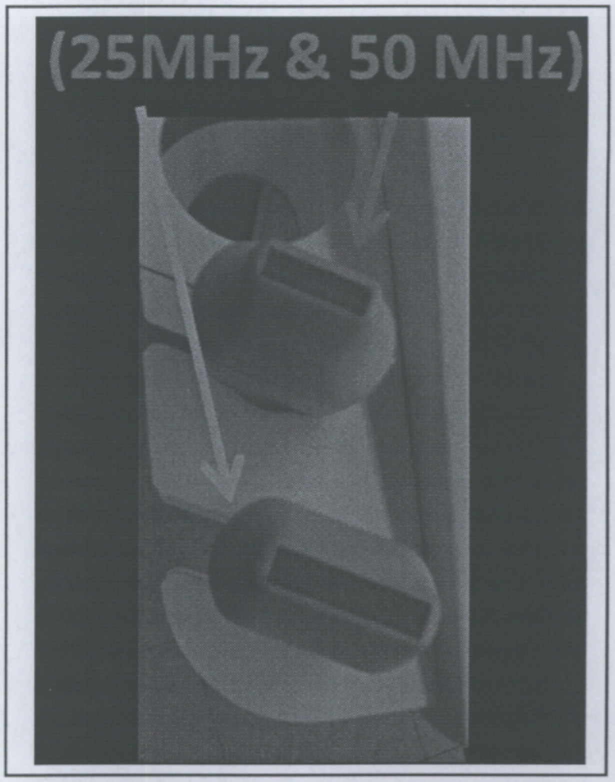

Figure 2. Displays the 50- and 25-MHz linear ultrasound arrays. MS550: depth resolution = 30 µm, lateral resolution = 90 µm, and slice thickness approximately 200 µm. MS250: depth resolution = 60 µm, lateral resolution = 150 µm, and slice thickness approximately 400 µm.

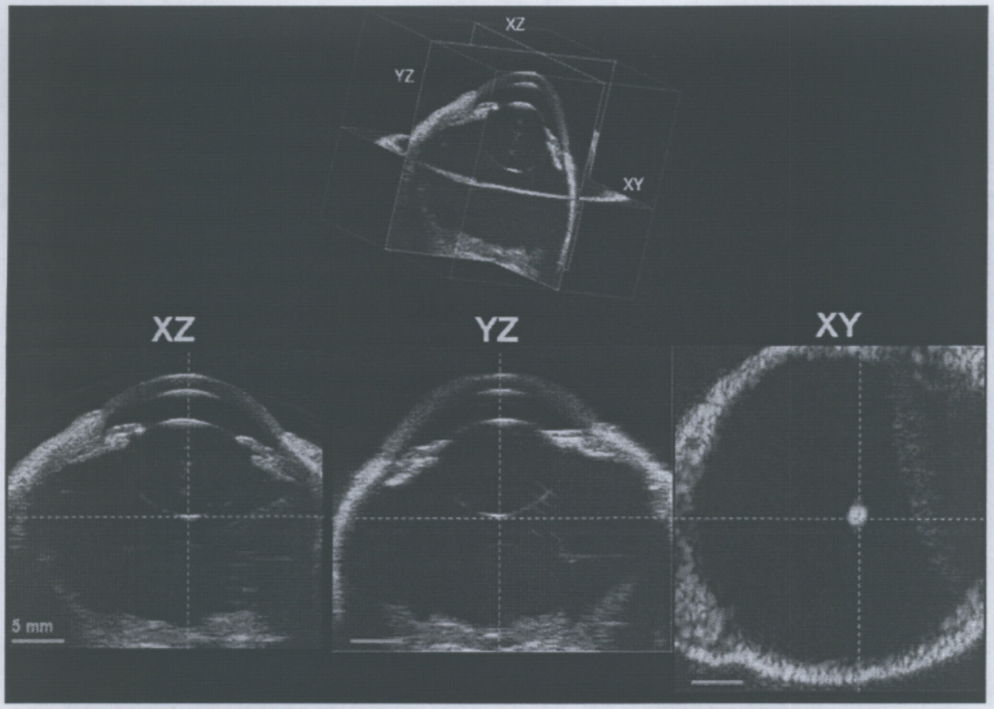

Figure 3. Two-dimensional orthogonal slices of a pig eye obtained with the 25-MHz probe and displayed with the Vevo 2100 scanner (VisualSonics, Toronto, Ontario, Canada). Note the anterior and posterior segment are imaged in three different sagittal, transverse, and coronal planes. A three-dimensional perspective is presented above the slices. Approximate spatial resolution: 60 µm (Z, axial), 150 µm (X, lateral), and 500 µm (Y, elevational/slice thickness).

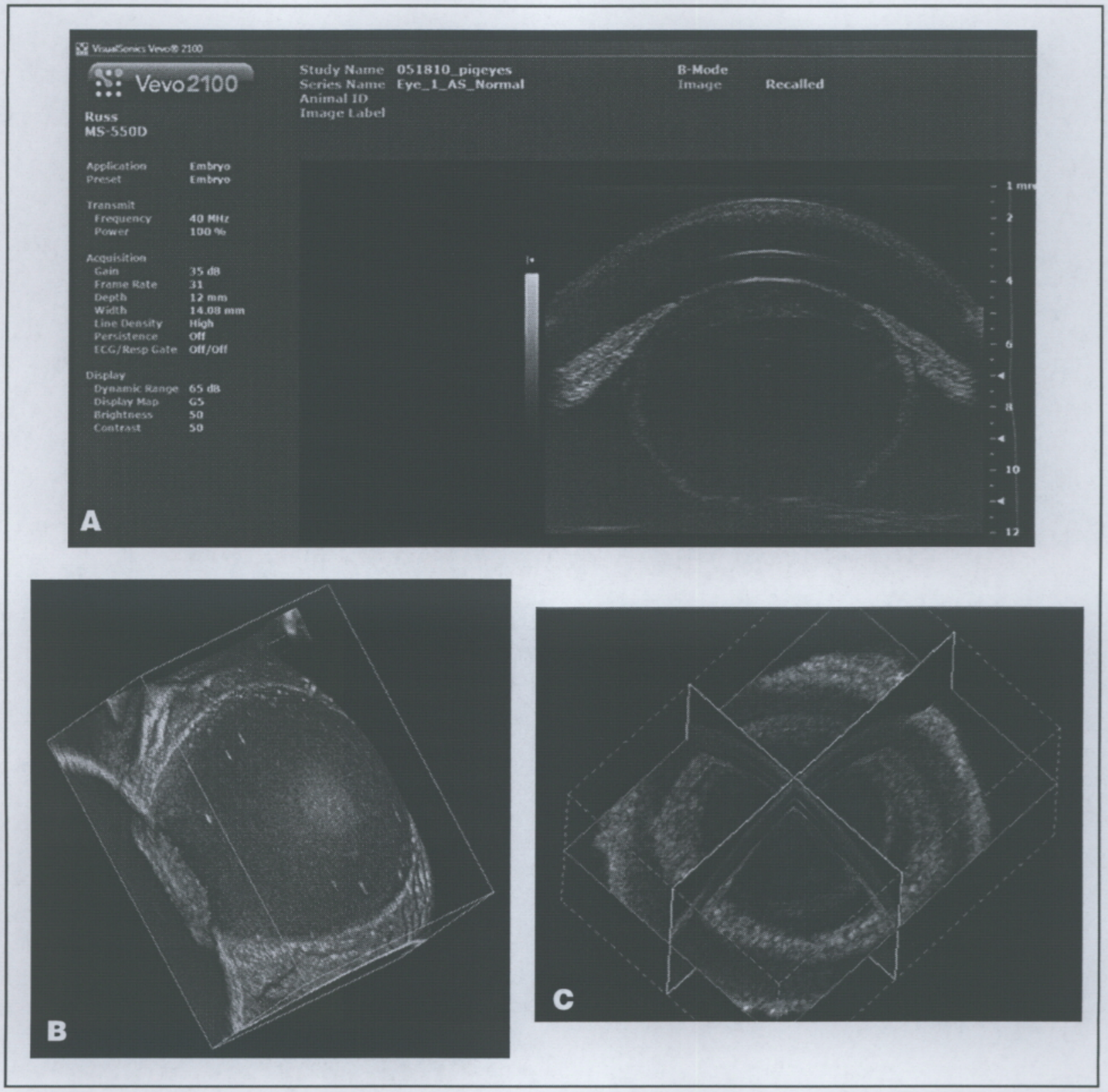

Figure 4. The 50-MHz images generated from the pig eyes exhibited superfine structures of the anterior segment in different planes (A to C). Figure 4B is a three-dimensional rendering of the cornea using the system. Approximate spatial resolution: 30 μm (Z, axial), 90 μm (X, lateral), and 200 μm (Y, elevational/slice thickness).

to automatically translate the transducer perpendicular to the B-mode imaging plane and collect a volumetric data set consisting of a series of cross-sectional slices of the eye. The built-in software allows the user to view any slice orientation or scroll through the entire 3D volumetric image within seconds of performing a scan (which generally takes 10 seconds for 3D). It can also make quantitative measurements of distances, angles, back scatter intensity, and volumes using a simple point-and-click interface. Finally, data can easily be exported to other software programs for further image processing, analysis, and display. The probes are normally coupled to tissue using standard ultrasound coupling gel (eg, Aquasonic 100; Parker Laboratories, Fairfield, NJ).

Method of Testing

For this preliminary study, we used the Vevo 2100 high-resolution ultrasonic unit for in vitro examination of

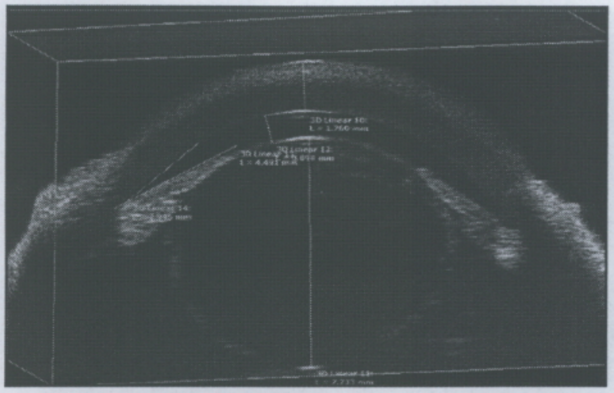

Figure 5. Two-dimensional image of the pig eye anterior segment using 50-MHz frequencies shows corneal thickness (1.760 mm), distance of the cornea from the lens surface (7.723 mm), thickness of the lens (0.898 mm), and the anterior chamber angle (2.945 mm).

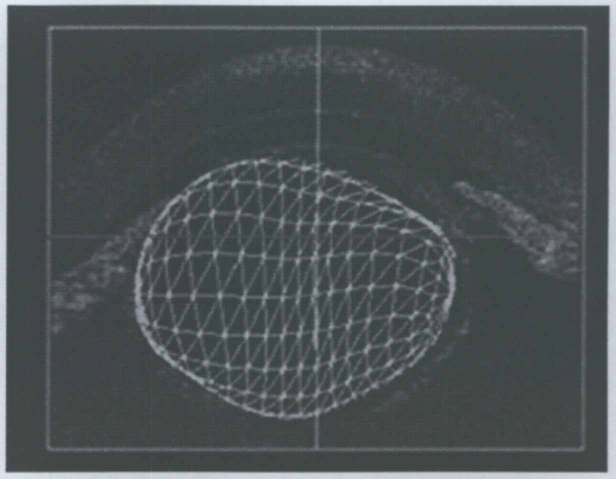

Figure 6. Displays volumetric measurement (pig eye) by outlining the lens capsule in different planes. The computer connects the meridionals and calculates the volume.

pig eyes and a limited in vivo examination of a human volunteer (GP) eye. No comparative investigation was performed with other commercial ultrasonic units. Pig eyes were obtained from a Colorado food abattoir and were kept on ice for transfer. Extraocular tissues were removed prior to ultrasonic examination. Eyes were either stabilized in a water bath by a custom holder or positioned in a cup covered with thick coupling gel. Eyes were scanned using both the 25- and 50-MHz probes. Some pig eyes were used to simulate lens injury or were implanted with an intraocular foreign body (ie, stainless steel needle).

We also scanned a human volunteer's eye with the 50-MHz probe through the eyelid after application of coupling gel on the eyelid surface. The volunteer was positioned horizontally and the automated transducer probe was aligned with the eye. An automated linear scan of the probe perpendicular to the B-mode imaging plane was controlled by the Vevo 2100 system. A single scan produced a 3D image. After scanning, the scanner permits rotation and display of the image on the monitor at any desired plane. The temporal arteries were also scanned in the human volunteer with the 50-MHz probe, and blood flow was visualized using the system's Color Doppler technology.

RESULTS

The 25-MHz probe revealed both the anterior and posterior structures of the pig eye (Fig. 3). The scan could be presented in 3D at different planes with sagittal, transverse, and coronal sections. Images could be recalled, rotated, or zoomed in for examination in any direction or slice projection. The 50-MHz images generated from the pig eyes exhibited superfine structures of the anterior segment in different planes (Fig. 4). The dimensions of the anterior segment structures and their distances from each other could be measured (Fig. 5). Similarly, we could calculate the anterior chamber angle and perform volumetric measurement of the crystalline lens (Fig. 6).

In pig eyes with traumatic lens injury, we could precisely locate the position, size of the injury, and its distance from the cornea (Fig. 7). Similarly, the location of the intraocular foreign body was imaged and localized in three different planes (Fig. 8).

Offline processing using image analysis software (Matlab; Mathworks, Natick, MA)—by clicking on a desired location on any image—simultaneously showed the images of that same area for the two remaining planes, thus providing an instantaneous view of a desired area in three different planes throughout the eye. This point-and-click technique made it possible to localize an intraocular foreign body and measure its location and dimensions (Fig. 8).

Ultrasonic examination of the human volunteer's eyes was done using the 50-MHz probe through the eyelid after applying a coupling gel. The ultrasonic images showed fine structures of the eyelid, including the Meibomian gland (Fig. 9), cornea, iris–ciliary body, and posterior capsule of the crystalline lens. All structures of the anterior segment could be individually analyzed. We also could image the temporal artery in high resolution and observe blood flow using the various Doppler modes (Fig. 10).

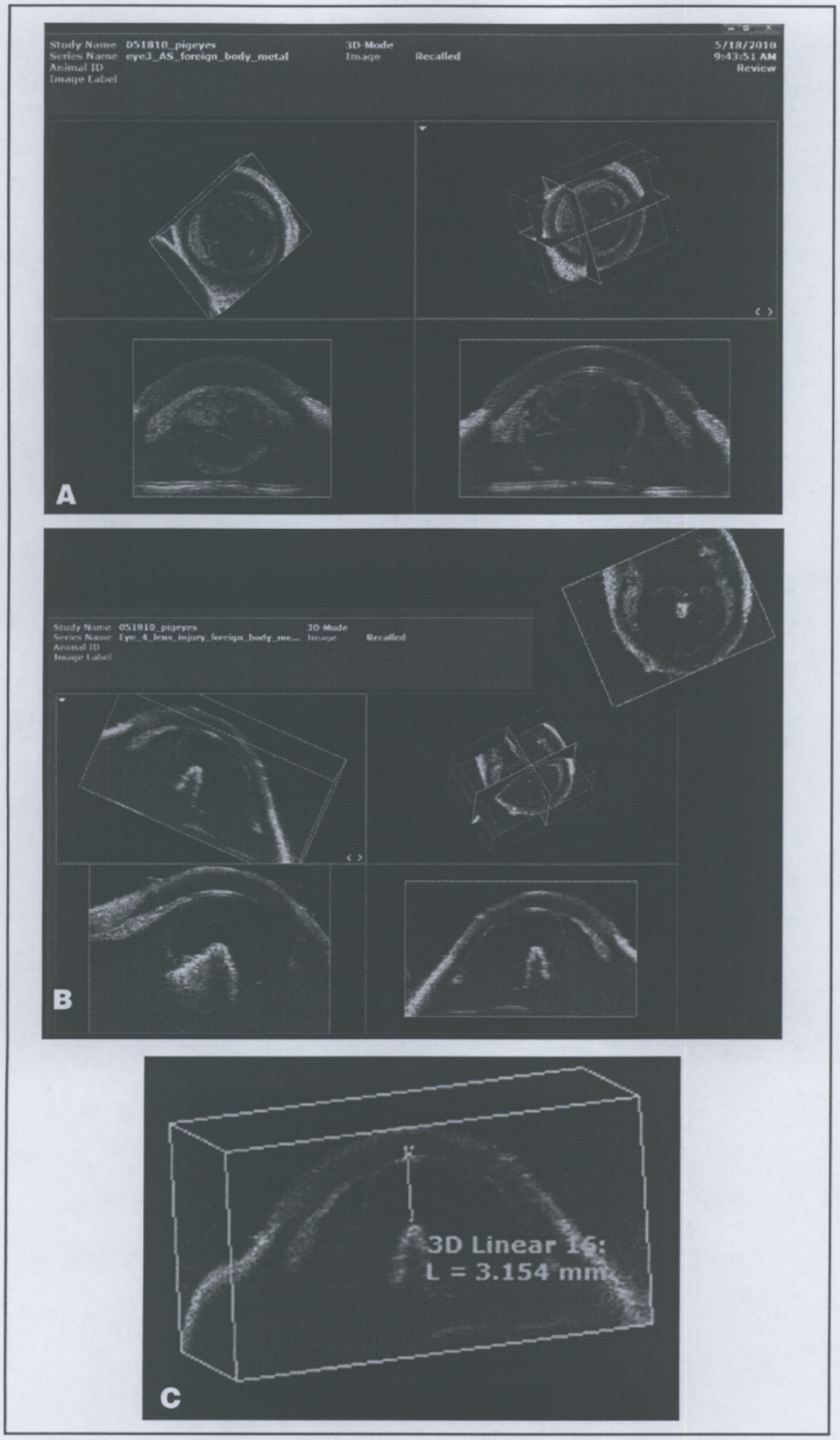

Figure 7. (A) Crystalline lens injury (pig eye) to the anterior lens capsule in different planes. (B) Posterior capsule injury seen in different planes. (C) Distance of the injury from the corneal endothelium (3.154 mm).

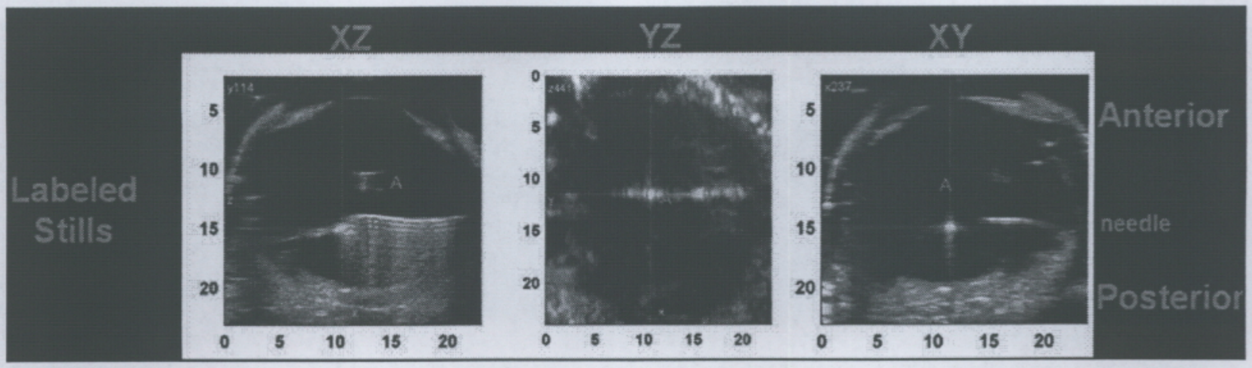

Figure 8. Two-dimensional image (pig eye) using a 25-MHz probe. Note the location of a long foreign body in the vitreous cavity with reverberating shadows below it in three different planes, obtained with the point-and-click technique. These images were generated offline using Matlab (Mathworks, Natick, MA).

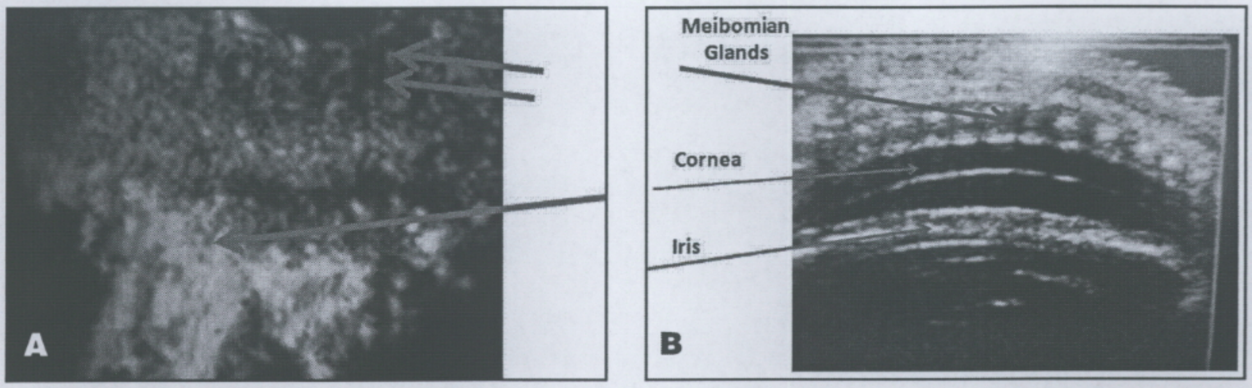

Figure 9. (A) Coronal section through the human superior eyelid shows dark lines of Meibomian glands using a 50-MHz probe. (B) The same as image A in cross-section shows dark spots of Meibomian glands surrounded by the gray–white images of the tarsal plate.

DISCUSSION

High-frequency ultrasonic linear arrays present a unique opportunity to examine the eye quickly and at high resolution (approximately 30 μm for the 50-MHz and 60 μm for the 25-MHz probe). Because 3D imaging of the eye with a linear array transducer is fast (approximately 10 seconds), this modality could potentially be used for an initial examination of a patient's eye. Having 3D images of the eye would reduce the chance of missing small lesions located in the iris–ciliary body regions. The examination would probably be easier on patients and more efficient for the examiner.

With some modifications, the dimension of the array transducer can be made large enough to cover the equatorial diameter of most normal eyes (> 25 mm with the probes currently offered by VisualSonics). The lower frequencies will also permit imaging of the posterior segment of myopic eyes and orbital tissue. In a routine examination, one can initially scan the anterior segment with the 50-MHz transducer (or higher frequency) followed immediately by a lower frequency scan to image the entire eye. The physician can obtain a preview of the entire eye using a cine-video in real-time 2D at 25-MHz ultrasound. One can measure the location, integrated backscatter, or dimensions of any structure, or do a complete volumetric analysis of a lesion or parts of the eye. On discovery of a lesion, volumetric studies can be performed by positioning the ultrasonic probe perpendicular to the lesion. Volumetric data could provide precise information on the growth of a lesion over time. Although the ideal condition for volumetric analysis of a lesion is to position the ultrasound perpendicular to it, routine examination using 3D ultrasound provides sufficient information regarding the presence or absence of pathology.

Although B-mode ultrasound has been useful in examination of traumatic eye injuries, one must be extremely cautious to avoid pressing the eye during the examination for fear of extruding the intraocular contents

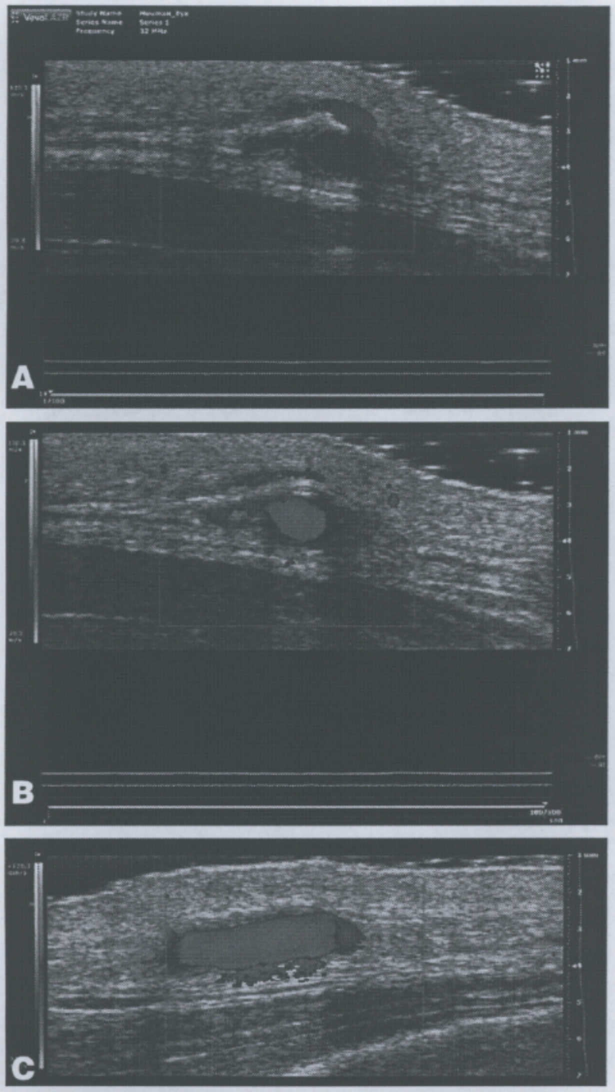

Figure 10. (A) Image of the cross-section of the human temporal artery using a 50-MHz probe. (B) Color Doppler image of blood flow in the temporal artery. (C) In-plane view, illustrating image of the blood flow in the temporal artery.

through a corneal wound. Examination of an eye with a manually positioned probe does not guarantee stability of the probe, even through the eyelid. The use of a water bath and eyelid speculum is not easy on an open eye with a penetrating corneal wound, although it may be indispensable for examination of the anterior segment. A time-consuming examination can be stressful for the patient. Because the array transducer moves automatically on a horizontal plane over the coupling agent and the closed eyelid, it reduces the chance of pressing on the eye. The array transducer also simplifies examination of the eye using the 50-MHz probe initially, and then is followed by use of the lower frequency probe (< 25 MHz). Complete data are available for analysis in a few seconds, and information obtained would be useful to diagnose the extent of traumatic eye injury and location of any potential intraocular foreign body.

The resolution of a structure depends on the frequency of the ultrasound. The resolution of two ultrasonic units at 50 MHz should be equal, but the software of the unit can facilitate improvement. If the current UBM unit is used with an 80-MHz probe, its resolution will be higher than the same unit with 50 MHz. However, the depth of the tissue to be scanned is reduced to less than 5 mm due to absorption of water at the higher frequencies.

The 50-MHz transducer provides high-resolution images (approximately 30 μm axial/depth, 90 μm lateral, and 300 μm elevation) of the anterior segment structures including the eyelid and Meibomian glands, which are rendered visible in various image planes (Fig. 9). Potentially, these images can provide additional anatomic and histologic-like information needed to evaluate patients with Meibomian gland disease.

The linear array transducers are also capable of simultaneously obtaining B-scan imaging and Color or Power Doppler. The Color Doppler capability of this unit was also used to examine the temporal artery in the volunteer subject. This modality provides an additional benefit in examination of patients with vascular diseases, such as temporal arteritis or vascular diseases affecting the optic nerve head.

It was not our intent to evaluate the Vevo 2100 for safety in a human eye. However, the unit provides information regarding the ultrasonic exposure in mechanical indices and is designed for safe exposure in small animals. The acoustic intensity employed for this study is comparable to other commercial units (mechanical indices < 1.2) for diagnostic ultrasound imaging.

The newly developed linear array high-resolution ultrasound unit is a versatile instrument that can provide exquisite images of the anterior and posterior segments of the eye through the eyelid in a short time. A shortcoming of this system is its high cost. Modification of this unit for ophthalmology may reduce the cost and will simplify routine examination of normal ocular structures or those affected by pathological processes, including intraocular tumor, retinal detachment, glaucoma, or ocular trauma. Doppler technology can also be used simultaneously in evaluation of blood flow in the temporal artery, assisting in evaluation of patients with suspected temporal arteritis.

Further clinical investigations and a comparative study with other commercial ultrasound ocular equipment must be performed to determine the potential benefit and feasibility of the Vevo 2100 for clinical use.

REFERENCES

1. Dussik KT. On the possibility of using ultrasound waves as a diagnostic aid [article in German]. *Z Neurol Psychiat.* 1942;174:153-168.
2. Elder I, Lindstrom K. The history of echocardiography. *Ultrasound Med Biol.* 2004;30:1565-1644.
3. Mundt GH Jr, Hughes WF Jr. Ultrasonics in ocular diagnosis. *Am J Ophthalmol.* 1956;41:488-498.
4. Oksala A, Lehtinen A. Diagnostic value of ultrasonics in ophthalmology [article in German]. *Ophthalmologica.* 1957;134:387-395.
5. Jansson F. Measurement of intraocular distances by ultrasound and comparison between optical and ultrasonic determination of the depth of the anterior chamber. *Acta Ophthalmol.* 1963;41:25-61.
6. Coleman DJ, Carlin B. A new system for visual axis measurements in the human eye using ultrasound. *Arch Ophthalmol.* 1967;77:124-127.
7. Oksala A, Lehtinen A. A measurement of the velocity of sound in some parts of the eye. *Acta Ophthalmol.* 1958;36:633-639.
8. Sanders DR, Kraff MC. Improvement of intraocular lens power calculation using empirical data. *J Am Intraocular Implant Soc.* 1980;6:263-267.
9. Ossoinig K. Clinical echo-ophthalmology. In: Blodi F, ed. *Current Concepts of Ophthalmology,* vol. III. St. Louis: Mosby; 1972.
10. Ossoinig K. The evaluation of kinetic properties of echo signals. In: Oksala A. Gernet H, eds. *Ultrasonics in Ophthalmology.* New York: Karger; 1967.
11. Baum G, Greenwood I. The application of ultrasonic locating techniques to ophthalmology. Part I: reflective properties. *Am J Ophthalmol.* 1958;46:319-329.
12. Baum G, Greenwood I. Ultrasonography: an aid in orbital tumor diagnosis. *Arch Ophthalmol.* 1960;64:180-194.
13. Baum G. Use of ultrasonography in the differential diagnosis of ocular tumors. In: Boniuk M, ed. *Ocular and Adnexal Tumors.* St. Louis: Mosby; 1964.
14. Purnell E. Ultrasound in ophthalmological diagnosis. In: Goldberg R, Sarin L, eds. *Diagnostic Ultrasound.* New York: Plenum Press; 1966.
15. Holasek E, Sokollu A. Direct contract, hand held, diagnostic B-scanner. *Proceedings IEEE Ultrasonics Symposium.* Boston: IEEE Computer Society; 1972:38-43.
16. Coleman DJ, Konig WF, Katz L. A hand-operated, ultrasound scan system for ophthalmic evaluation. *Am J Ophthalmol.* 1969;68:256-263.
17. Bronson NR. Development of a simple B-scan ultrasonoscope. *Trans Am Ophthalmol Soc.* 1972;70:365-408.
18. Fisher YL, Bronson NR, Schutz JS, Llovera IN. Contact B-scan ultrasonography: clinicopathological correlations. *Ann Ophthalmol.* 1975;7:779-786.
19. Oksala A. Echogram in melanoma of the choroid. *Br J Ophthalmol.* 1959;43:408-414.
20. Oksala A. Ultrasound diagnosis in intraocular melanomas. *Ann N Y Acad Sci.* 1963;100:18-28.
21. Ossoinig K, Till P. Methods and results of ultrasonography in diagnosing intraocular tumors. In: K. Gitter et al., ed. *Ophthalmic Ultrasound.* St. Louis: Mosby; 1969.
22. Poujol J. Clinical echography in intraocular tumors. In: Bock J and Ossoinig K, eds. *Ultrasonographica Medica (SIDUO III).* Vienna: Verlag der Weiner Med Akad; 1971.
23. Baum G. Ultrasonographic characteristics of malignant melanoma. *Arch Ophthalmol.* 1967;78:12-15.
24. Silverman RH, Coleman DJ, Rondeau MJ, Woods SM, Lizzi FL. Measurement of ocular tumor volumes from serial, cross-sectional ultrasound scans. *Retina.* 1993;13:69-74.
25. Coleman DJ, Silverman RH, Rondeau MJ, Lizzi FL. New perspectives: 3-D volume rendering of ocular tumors. *Acta Ophthalmol Suppl.* 1992;204:22.
26. Coleman DJ. Reliability of ocular and orbital diagnosis with B-scan ultrasound. I: Ocular diagnosis. *Am J Ophthalmol.* 1972;73:501-516.
27. Coleman DJ. Reliability of ocular and orbital diagnosis with B-scan ultrasound. II: Orbital diagnosis. *Am J Ophthalmol.* 1972;74:704-718.
28. Coleman DJ, Lucas BC, Rondeau MJ, Chang S. Management of intraocular foreign bodies. *Ophthalmology.* 1987;94:1647-1653.
29. Bronson NR 2nd. Management of intraocular foreign bodies. *Int Ophthalmol Clin.* 1974;14:129-150.
30. Purnell E. Ultrasonic interpretation of orbital disease. In: Gitter K, et al., eds. *Ophthalmic Ultrasound.* St. Louis: Mosby; 1969.
31. Coleman DJ, Jack RL, Franzen LA. Ultrasonography in ocular trauma. *Am J Ophthalmol.* 1973;75:279-288.
32. Pavlin CJ, Sherar MD, Foster FS. Subsurface ultrasound microscopic imaging of the intact eye. *Ophthalmology.* 1990;97:244-250.
33. Pavlin CJ, Harasiewiecz K, Sherar MD, Foster FS. Clinical use of ultrasound microscopy. *Ophthalmology.* 1991;98:287-295.
34. Pavlin CJ, Foster FS. Ultrasound biomicroscopy: high frequency ultrasound imaging of the eye at microscopic resolution. *Radiol Clin North Am.* 1998;36:1047-1058.
35. Foster FS, Pavlin CJ, Harasiewicz KA, Christopher DA, Turnbull DH. Advances in ultrasound biomicroscopy. *Ultrasound Med Biol.* 2000;26:1-27.
36. Reinstein DZ, Silverman RH, Raevsky T, et al. Arc-scanning very high frequency digital ultrasound for 3-D pachymetric mapping of the corneal epithelium and stroma in laser in situ keratmileusis. *J Refract Surg.* 2000;16:414-430.
37. Coleman DJ, Fish SK. Presbyopia accommodation, and the mature catenary. *Ophthalmology.* 2001;108:1544-1551.
38. Silverman RH, Lizzi FL, Ursea BG, et al. High resolution imaging and characterization of the ciliary body. *Invest Ophthalmol Vis Sci.* 2001;42:885-894.
39. Cusumano A, Coleman DJ, Silverman RH, et al. Three dimensional ultrasound imaging: clinical applications. *Ophthalmology.* 1998;105:300-306.
40. Fisher Y, Hanutsaha P, Tong S, Fenster A, Mazarin G, Mandava N. Three dimensional ophthalmic contact B-scan ultrasonography of the posterior segment. *Retina.* 1998;18:251-256.
41. Ennezat PV, Logeart D, Berrebi A, Vincentelli A, Maréchaux S. Key role Doppler echography in the emergency management of elderly patients. *Arch Cardiovasc Dis.* 2010;103:115-128.
42. Wells PM. Ultrasonic colour flow imaging. *Phys Med Biol.* 1994;39:2113-2145.
43. Guerriero S, Alcazar JL, Ajossa S, et al. Transvaginal color Doppler imaging in detection of ovarian cancer in a large study population. *Int J Gynecol Cancer.* 2010;20:781-786.
44. Plange N, Remky A, Arend KO. Potential diagnostic value of fluorescein angiography and color Doppler imaging in primary open angle glaucoma. *Eur J Ophthalmol.* 2010;20:1091-1092.
45. AbuRahma AF, Srivastava M, Stone PA, et al. Critical appraisal of the carotid Duplex Concensus criteria in the diagnosis of the carotid artery stenosis. *J Vasc Surg.* 2011;53:53-59.
46. Macsweeney JE, Cosgrove DO, Arenson J. Color Doppler energy (power) mode ultrasound. *Clin Radiol.* 1996;51:387-390.
47. Yamamoto Y. Doppler examination of blood flow in the ocular fundus. *Bibl Ophthalmol.* 1975;83:32-40.
48. Dennis KJ, Dixon RD, Winsberg F, Ernest JT, Goldstick TK. Variability in measurement of central retinal artery velocity using color Doppler imaging. *J Ultrasound Med.* 1995;14:463-466.
49. Susal AL, Gavnon MW, Walker JT. Linear array multiple transducer ultrasonic examination of the eye. *Ophthalmology.* 1983;90:266-271.
50. Blaivas M, Theodoro D, Sierzenski PR. A study of bedside ocular ultrasonography in the emergency department. *Acad Emerg Med.* 2002;9:791-799.
51. Cannata JM, Williams JA, Zhou QF, et al. Development of a 35-MHz piezo-composite ultrasound array for medical imaging. *IEEE Transactions on Ultrasonics Ferroelectrics and Frequency Control.* 2006;53:224-236.